Desalination and Water Treatment
www.deswater.com

doi: 10.5004/dwt.2022.28805

270 (2022) 172–184
September

Synthesis of polyethylenimine modified sugarcane bagasse cellulose and its competitive adsorption of Pb^{2+}, Cu^{2+} and Zn^{2+} from aqueous solutions

Wenyan Jiang[a], Yihao Xing[b,†], Leixing Mo[a], Jie Liao[a], Wei Chen[a], Haijun Wang[a], Tianshun Wang[a,*]

[a]*Agro-Products Quality Safety and Testing Technology Research Institute, Guangxi Academy of Agricultural Sciences, Nanning 530007, China, Tel. +8607713899306; emails: wangts@gxaas.net (T. Wang), duanmuzheng2010@163.com (W. Jiang), molx@163.com (L. Mo), liao_jie1997@163.com (J. Liao), 373827366@qq.com (W. Chen), 837063255@qq.com (H. Wang)*
[b]*Genebank of Guangxi Academy of Agricultural Sciences, Nanning 530007, China, Tel. +8607713245087; email: yh_xing@126.com (Y. Xing)*

Received 25 March 2022; Accepted 3 August 2022

ABSTRACT

In this study, a new biosorbent was prepared from sugarcane bagasse and polyethylenimine (MSCP). The effects of preparation parameters, including the polyethylenimine (PEI) concentration, the glutaraldehyde concentration, the reaction temperature, and ball milling time on the adsorption property of MSCP were studied. The optimum preparation conditions were as follows: the PEI concentration was 20%, the glutaraldehyde concentration was 2.0%, the reaction temperature was 318.15 K, and the ball milling time was 20 min. Under the optimum preparation conditions, the removal efficiency of Cu^{2+} by MSCP was reached 93.3%. The physical and chemical properties of MSCP were determined by scanning electron microscopy (SEM), Fourier-transform infrared spectroscopy (FTIR) and elemental analysis. The SEM micrographs revealed that surface morphology of MSCP was rough, with many irregular folds and small particles. The FTIR and elemental analysis results indicated PEI was successfully grafted to the surface of sugarcane bagasse cellulose (SC) with glutaraldehyde as a bridge and the adsorption mechanism of heavy metals by MSCP can be regarded as the complexation between heavy metals and $–NH_2$ groups of MSCP. Langmuir model showed the best fitting to the isotherm equilibrium data, the maximum adsorption capacities for Cu^{2+}, Pb^{2+} and Zn^{2+} were 114.02, 165.56 and 95.79 mg/g, respectively. The adsorption experimental data were fitted well by pseudo-second-order. In multi-solute system, the competitive adsorption ability of heavy metals by MSCP followed the order of $Pb^{2+} > Cu^{2+} > Zn^{2+}$.

Keywords: Synthesis; Competitive adsorption; Polyethylenimine; Sugarcane bagasse

1. Introduction

Wastewater containing heavy metals is generally discharged from electroplating, metal processing, textile, mining, glass and other industries [1]. Unlike organic pollutants, heavy metals are non-biodegradable persistent pollutants that tend to accumulate in organisms and enter the food chains. Heavy metals from industrial wastewater are toxic to organisms, especially, excessive presence of Pb, Cu and Zn in wastewater may have a destructive effect on human immune system and lead to cancers [2,3]. In addition, due to the common source and co-treatment of wastewater, multiple heavy metals often coexist in sewage [4]. For example, during copper mining and ore

* Corresponding author.

† Equivalent contribution author.

dressing, both Pb and Zn are discharged into the ecological environment [5]. The coexistence of heavy metals from wastewater indicates that it is necessary to study their competitive adsorption and migration characteristics [6]. In multiple heavy metals systems, the adsorption of heavy metal ions not only related to the surface characteristics of the adsorbent and the physicochemical parameters of the solution, but also related to the characteristics of these heavy metals [7].

Many methods have been reported for the removal of heavy metals, including chemical precipitation, ion exchange, reverse osmosis, coagulation and flocculation, membrane separation [8,9]. Most of these methods are costlier and lead to the formation of by-products, or they are less efficient. Therefore, it is very important to find a more suitable and convenient method to treat wastewater containing heavy metals [10]. Among the available technologies, adsorption technology is considered as one of the technologies for treating wastewater containing heavy metals, because it has the characteristics of simple design, easy operation, low application cost and wide application range [11,12]. Many different sources of adsorbents are used to remove heavy metals from wastewater. Most of these materials are abundant and readily available, such as agricultural by-products or other industrial wastes [13]. Among these materials, biomass-based adsorbents such as olive seed, bamboo powder, coconut shell, peanut shell, straw, and sugarcane bagasse (SB) are expected to be new materials for wastewater treatment due to their low cost and small environmental burden [14–16].

The agricultural wastes in general mainly composed of cellulose, hemicellulose and lignin, which contain many hydroxyl and hydroxymethyl groups that can be transformed into other functional groups by oxidation and other reactions, thus showing a high potential biosorption capacity [17]. Although many agricultural wastes may be used to produce cellulose, there are significant economic advantages in producing cellulose materials from sugarcane bagasse (SB). Compared to other agricultural wastes, SB does not require a higher cost of collection and transportation. SB concentrated in sugar mills, is a low-value agricultural wastes that produced 1.6 billion tons of SB annually worldwide in 2011 [18]. Although bagasse is rich in cellulose (40%–50%) and hemicellulose (25%–30%) and shows certain adsorption capacity to heavy metals, the adsorption capacities of the unmodified SB for heavy metals are low because the number of functional groups on the surface was not sufficient to remove heavy metals. Therefore, to improve the adsorption capacity of SB for heavy metals, physical or chemical methods should be used to modify it to increase the content of functional groups, so as to improve its metal adsorption capacities. Esterification, etherification, halogenation, oxidation and chemical grafting modification have been applied to improve the metal ion binding capacity of cellulose materials [19,20]. The treatment of wastewater containing heavy metals by chemically modified SB has been reported in various literatures. Nashine and Tembhurkar [21] reported the adsorption of As(III) by iron oxide impregnated sugarcane bagasse. Ai et al. [17] analyzed the adsorption of Cd^{2+} by using sugarcane bagasse treated with nitric acid.

It is well known that hydrazine, amine and thiamine groups have excellent removal effect on pollutants in wastewater, which can not only adsorption of cationic metal ions through chelation, but also remove anions by electrostatic action [22,23]. Polyethylenimine (PEI) is a cationic polyelectrolyte containing many amino groups, which shows strong adsorption capacity for Cu^{2+}, Cd^{2+}, and Zn^{2+} by complexation or electrostatic interaction [24–26]. Jiang et al. [27] used PEI-functionalized magnetic nanoparticles to remove Pb(II), and the results showed that MNPs@PEI had good reuse performance and practical application potential. Liu et al. [28] synthesized polyethylenimine (PEI)/graphene oxide (GO) to remove U(VI) from wastewater, and the adsorbent exhibited a high removal efficiency for U(VI).

Ball milling is a method of changing the crystal structure of materials by friction, collision, shear or other mechanical action [29]. At present, ball milling is widely used in the preparation of nanocellulose due to its simple operation and relatively cheap equipment [30,31]. Therefore, it is promising to use the ball milling method to synthesize cellulose materials.

As a consequence, the use of sugarcane bagasse cellulose as supporting material can not only significantly reduce the need for traditional agricultural waste disposal and the production costs, but also make full use of easily available agricultural resources. The crystalline structure of bagasse cellulose was destroyed by ball milling, which made cellulose more easily dissolved in 7 wt.% NaOH/12 wt.% urea aqueous solution. Grafting branched PEI using glutaraldehyde crosslinking method has been reported to be an easy and cheap method of introducing amino groups. After sugarcane bagasse cellulose is grafted with PEI, the prepared material would have a large number of amino groups and the adsorption capacity of adsorbent would be enhanced to a great extent due to the amino chelating effect with certain heavy metal ions. Therefore, the modified sugarcane bagasse cellulose as an inexpensive and efficient adsorbent provides a promising alternative for heavy metals contaminated wastewater treatment from the view of sustainability.

For this purpose, the ball milling method was introduced to synthesize sugarcane bagasse cellulose, and polyethylenimine was used to modify the cellulose to obtain a material with high adsorption capacity for heavy metals. The prepared adsorbent was characterized by scanning electron microscopy (SEM), Fourier-transform infrared spectroscopy (FTIR), Brunauer–Emmett–Teller (BET) and elemental analysis. The effects of preparation parameters, including the PEI concentration, the glutaraldehyde concentration, the reaction temperature, and ball milling time on the adsorption property of the adsorbent were investigated. The competitive adsorption property of Cu^{2+}, Pb^{2+} and Zn^{2+} was also studied.

2. Experimental

2.1. Materials

SB was obtained from Sugarcane Research Institute, Guangxi Academy of Agricultural Sciences (Guangxi, China). Polyethylenimine (PEI), glutaraldehyde, $Cu(NO_3)_2 \times 3H_2O$,

$Pb(NO_3)_2$ and $Zn(NO_3)_2{\times}6H_2O$ were of analytical reagent grade.

2.2. Synthesis of the adsorbent via the PEI cationic modification of SB

2.2.1. SB treatment

In this study, the lignin and other components of sugarcane bagasse were removed by acid-base pretreatment to prepare sugarcane bagasse cellulose (SC) according to our previous work [32]. In brief, SB was treated with 8% nitric acid solution (the ratio of SB and HNO_3 solution is 1:100 [g/mL]) at the temperature of 353.15 K for 3 h, and the mixture was washed in distilled water until neutral. Then, the acid-treated SB and 1.0 g anhydrous sodium sulfite were added to 2.5% NaOH (100 mL) solution. The mixture was stirred for 3 h at the temperature of 353.15 K and washed in distilled water until neutral. The base treated SB was boiled for 1 h with 1% sodium sulfite solution (100 mL) and washed to neutral with distilled water, then washed with acetone and dried in the oven get SC. Finally, mechanically activated sugarcane bagasse cellulose (MSC) was obtained by using ball milling technology to treat SC (the ball time ranged from 0 to 30 min).

2.2.2. Preparation of PEI modification of MSC

According to Qi et al. [33], MSC was rapidly dissolved in 7 wt.% NaOH/12 wt.% urea solution at low temperature (261.15 K) to obtain 1.0 wt.% solution. Then 5 mL PEI (10 wt.%–40 wt.%) and was 20 mL glutaraldehyde (1.5 wt.%–3.5 wt.%) added into MSC solution and stirred mechanically for 3 h at the desired temperatures (298.15–338.15 K). Finally, the suspension was filtered to obtain the orange solid sample. The sample was washed with distilled water 5 times to remove the residual urea, NaOH and PEI, and dried at 323.15 K and then ground to obtain the required MSCP powder.

2.3. Characterization

The surface micro-morphology of the sample was studied by the scanning electron microscope (SEM, Quanta 400 FEG, America). The functional groups of the sample were analyzed by Fourier-transform infrared spectrometer (FTIR, Nicolet 6700, America). The mass ratios of C, H and N of the sample were analyzed by Elemental Analyzer (Vario EL Cube, Elementar Co., Germany). The specific areas of adsorbents were characterized using BET method by a Micromeritics Gemini apparatus (ASAP 2020 M+C, Micromeritics, Co., USA)

The determination of zero charge point (pH_{pzc}) refers to the research method of Djebri et al. [34]. In brief, 0.02 g MSCP was added to 50 mL of 0.02 M sodium chloride solution with different pH values to oscillate. The initial pH ($pH_{initial}$) was adjusted between 2 and 8 by using 0.1 M hydrochloric acid or sodium chloride solution. The final pH value of the solution (pH_{final}) was determined after stirred mechanically for 48 h at 298.15 K. The pH_{pzc} was derived from the plot of pH_{final} vs. $pH_{initial}$.

2.4. Adsorption experiments

0.05 g MSCP and 50 mL Cu^{2+} solution with an initial concentration of 30 mg/L were added to the conical flask. The solution pH was adjusted to 5 and the suspension was shaken in a thermostatic oscillator at 154 rpm for 12 h. After the adsorption was completed, the suspension was withdrawn and rapidly filtered, and the concentration of Cu^{2+} was analyzed by Atomic Absorption Spectrometer (AA900T, PE, USA). The removal efficiency of heavy metal ion (η, %) and the adsorption capacity of heavy metal ion adsorbed by adsorbent at equilibrium (q_e, mg/g) were calculated by Eqs. (1) and (2), respectively.

$$\eta(\%) = \frac{C_0 - C_t}{C_0} \times 100\% \tag{1}$$

$$q_e = \frac{C_0 - C_e}{m} \times V \tag{2}$$

where C_0 (mg/L) and C_t (mg/L) are the initial concentration and the concentration of Cu^{2+} at sampling time t respectively; C_e (mg/L) is the equilibrium concentration of heavy metal ion; V (mL) is the volume of the sample; m (g) is MSCP dosage.

2.5. Adsorption isotherms

The adsorption capacities of MSCP at 298.15 K were measured using the following procedure. Cu^{2+}, Pb^{2+} and Zn^{2+} solutions were configured into a series of working solutions with different concentrations (20 to 240 mg/L). In addition, 0.03 g of MSCP was added into 50 mL of operational solution and the suspension was in a thermostatic oscillator at 154 rpm for 12 h The MSCP were removed by filtration, and the filtrates were collected to measure the final ion concentration by Atomic Absorption Spectrometer (AA900T, PE, USA).

2.6. Adsorption kinetics

0.03 g MSCP and 50 mL of 30 mg/L Cu^{2+}, Pb^{2+} and Zn^{2+} working solutions were added separately in the conical flask, and then the solutions were shaken on a thermostatic oscillator at 298.15 K for 6.5 h. The solutions were taken at different time intervals, and the concentration variations of metal ions were analyzed using Atomic Absorption Spectrometer (AA900T, PE, USA).

2.7. Competitive adsorption experiments

0.03 g MSCP and 50 mL of heavy metal ions solution was placed in a 250 mL conical flask. The initial concentrations of solutions containing multiple heavy metal ions (Cu^{2+}, Pb^{2+} and Zn^{2+}) are shown in Table 1. The mixture was shaken in a thermostatic oscillator (154 rpm) for 6.5 h at 298.15 K. After the adsorption was completed, the suspension was withdrawn and rapidly filtered, and the concentrations of Cu^{2+}, Pb^{2+} and Zn^{2+} were analyzed by Atomic Absorption Spectrometer (AA900T, PE, USA). The distribution coefficient (K_d) was calculated by Eq. (3):

Table 1
Metal solutions used to study competitive adsorption experiments

System	Solution
Single	20~80 mg/L Cu^{2+},
	20~80 mg/L Zn^{2+}
	20~80 mg/L Pb^{2+}
Binary	20~80 mg/L Cu^{2+} + 20~80 mg/L Zn^{2+}
	20~80 mg/L Cu^{2+} + 20~80 mg/L Pb^{2+}
	20~80 mg/L Zn^{2+} + 20~80 mg/L Pb^{2+}
Ternary	20~80 mg/L Cu^{2+} + 20~80 mg/L Zn^{2+} + 20~80 mg/L Pb^{2+}

$$K_d = \frac{(C_0 - C_e)V}{mC_e} \quad (3)$$

3. Results and discussion

3.1. Characterization of MSCP

Before and after adsorption of Cu^{2+} by MSCP were defined as $MSCP_{BAD}$ and $MSCP_{AAD}$, respectively. The SEM picture of SC (Fig. 1a), MSC (Fig. 1b), and $MSCP_{BAD}$ (Fig. 1c) and $MSCP_{AAD}$ (Fig. 1d) are represented in Fig. 1, and the SEM pictures of all the samples were amplified by 5,000 times. Fig. 1a shows that the surface of SC was compact and smooth without pores. Compared with SC, the surface of MSC was rougher than that of SC. The reason is that after the ball milling of SC, the crystalline structure of cellulose was destroyed and the degree of crystallinity of cellulose was also decreased. Fig. 1c shows that the surface of MSCP was rough, with many irregular folds and small particles. After MSCP adsorbed Cu^{2+}, the main structure of MSCP did not change much, and many regular granular white particles can be seen on the surface of MSCP, indicated

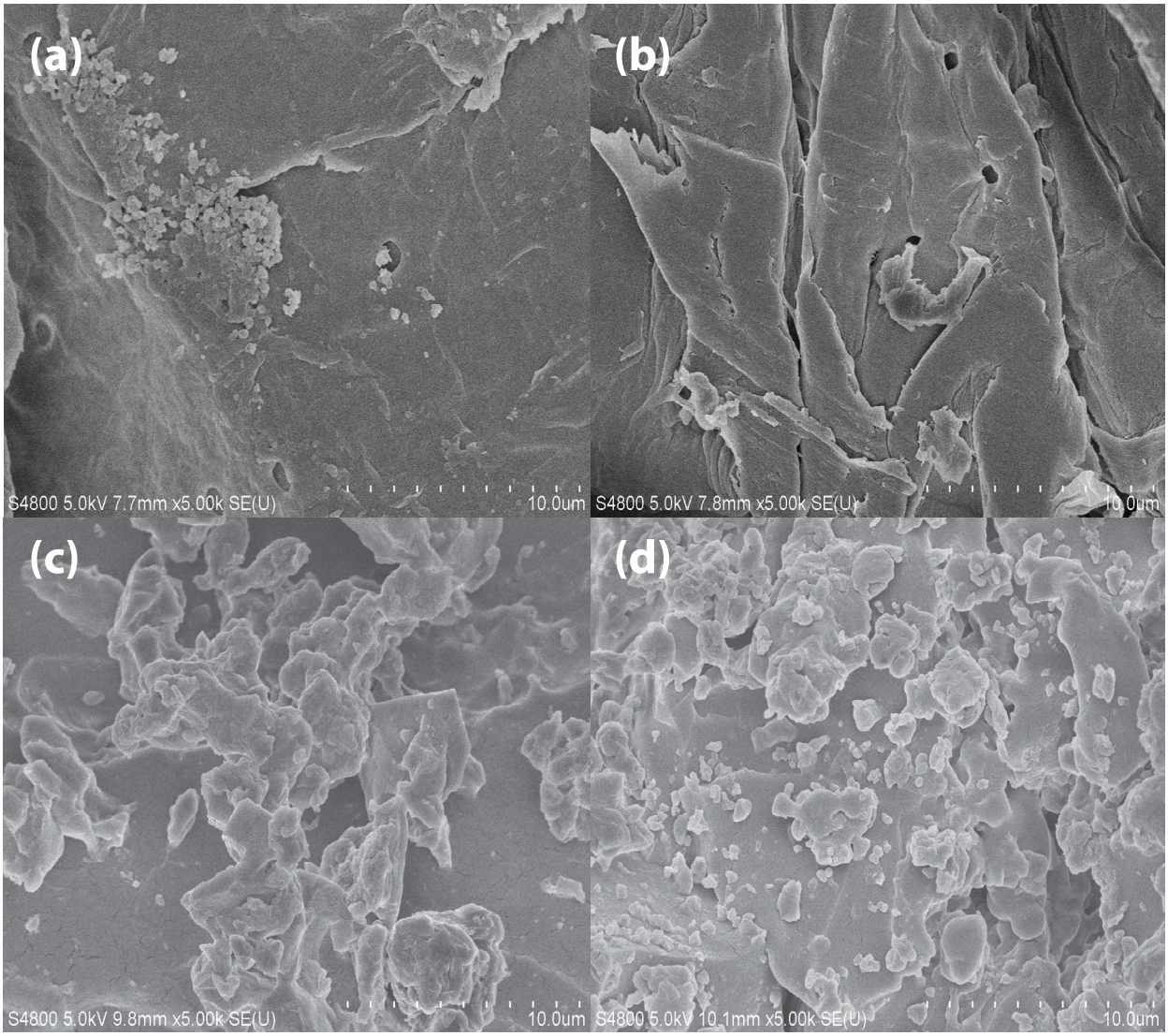

Fig. 1. SEM picture of (a) SC, (b) MSC, (c) $MSCP_{BAD}$, and (d) $MSCP_{AAD}$.

that the adsorption process had occurred. Successive BET analysis has shown that MSCP predominately a mesoporous material with average pore diameter of 9.2 nm, but with very low porosity. Determined specific BET surface area was just 2.907 m^2/g. After MSCP adsorbed Cu^{2+}, BET specific surface area was 2.373 m^2/g, which showed little change. Based on the results, it can be seen that nano pores of MSCP do not play significant role in Cu^{2+} adsorption.

The FTIR spectra of SC and $MSCP_{BAD}$ and $MSCP_{AAD}$ are shown in Fig. 2. The FTIR spectra of SC show that the wide and strong bands in the range of 3,200~3,600 cm^{-1} correspond to the stretching vibration bands of –OH. The absorbing peak emerged at 2,902 cm^{-1}, implying the asymmetric tension and vibration of $–CH_2$. The absorbing peak appeared at 1,637 cm^{-1} was related to the vibration and bending of –COOH. The peaks from 1,165 to 1,029 cm^{-1} corresponding to the stretching of C–O bond on the cellulose [35]. After cationic modification by PEI, it was observed from FTIR spectra of MSCP that the wide band at 3,447 cm^{-1} was due to the overlap of N–H and O–H stretching vibrations [36,37]. Moreover, a new peak observed at 1,471 cm^{-1} in the FTIR spectra of MSCP, it is the typical deformation pattern of the hydroxyl group on the cellulose binding to the $–NH_2$ group on PEI [38]. After MSCP adsorbed Cu^{2+}, the absorption band of NH_2 at 1,471 cm^{-1} disappeared and the peaks of OH bending vibration at 1,314 cm^{-1} shifted to 1,384 cm^{-1} in FTIR spectra of $MSCP_{AAD}$. Those results showed that the glutaraldehyde serves as a bridge to graft the PEI onto the MSCP surface, and nitrogen atoms of NH groups are the adsorption sites of MSCP for Cu^{2+} adsorption. Then the possible complex mechanism is shown in Fig. 3.

The contents of C, N and H in SC and MSCP are shown in Table 2. After PEI modification, the nitrogen content of MSCP increased significantly from 0.44% to 14.70%, which may be related to the introduction of amino groups on PEI to SC surface, thus increasing the content of N element in MSCP. The results of elemental analysis and FTIR spectra both confirmed that PEI was successfully grafted onto SC.

As shown in Fig. 4, pH_{pzc} of MSCP calculated as 2.47 based on the plot of pH_{final} vs. $pH_{initial}$. When the solution pH > pH_{pzc}, MSCP surface was negatively charged, which

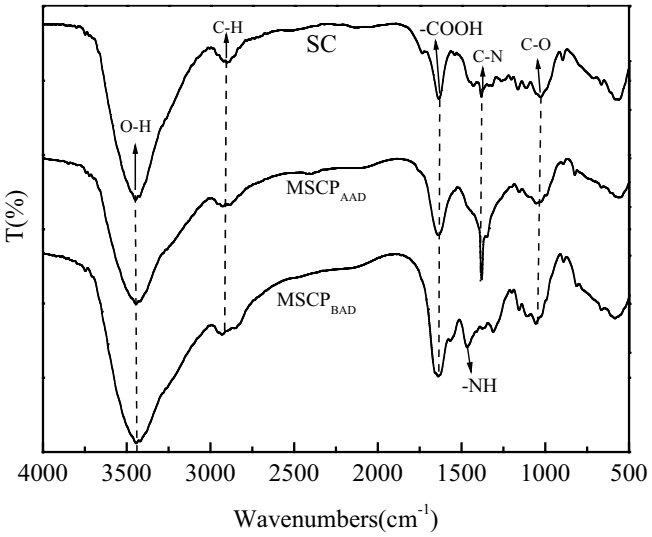

Fig. 2. FTIR of SC, $MSCP_{BAD}$, and $MSCP_{AAD}$.

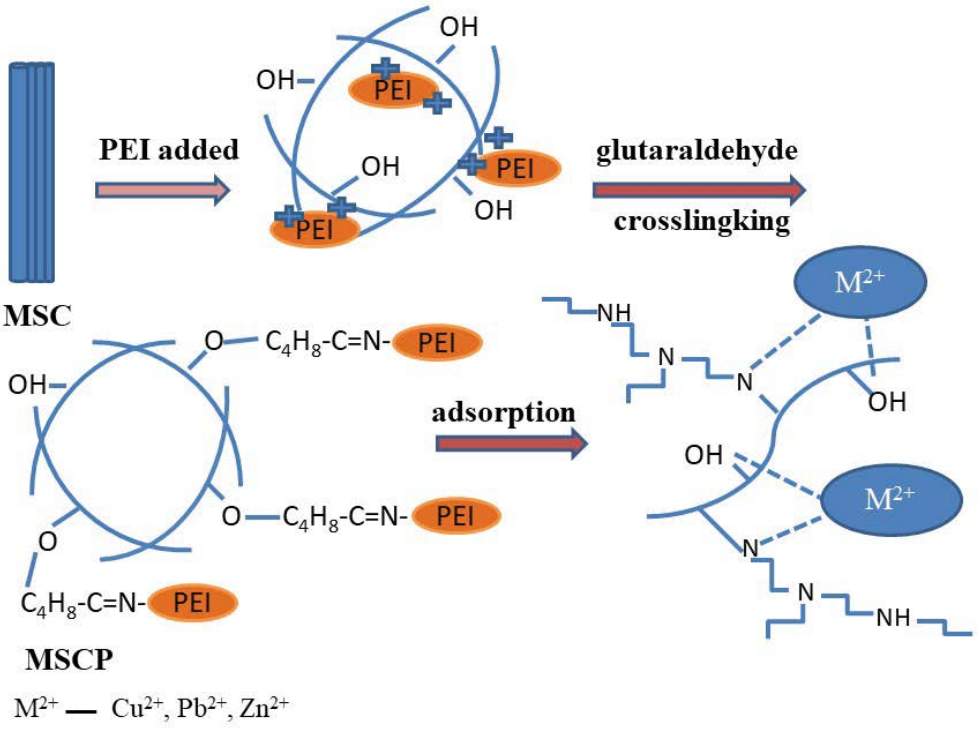

Fig. 3. The possible adsorption mechanism of metals by MSCP.

Table 2
C, H, N contents in the SC and MSCP

Sample	C (%)	H (%)	N (%)
SC	45.42	5.98	0.44
MSCP	41.35	7.15	14.70

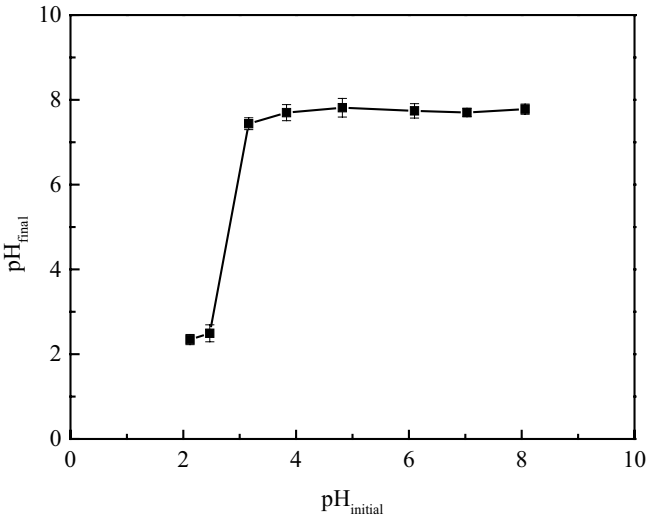

Fig. 4. Initial vs. final pH plot for the determination of zero point charge of MSCP.

was conducive to the adsorption of positively charged metal ions by electrostatic attraction [39]. When the solution pH < pH_{pzc}, MSCP surface was positively charged, and the concentration of H^+ is relatively high. A large number of H^+ and positively charged metal ions compete for empty adsorption sites, resulting in the reduction of metal ion adsorption capacity [40]. Therefore, heavy metals adsorption onto MSCP is favored at pH value higher than pH_{pzc} [41–42]. The knowledge about of pH_{pzc} may indicate the possible electrostatic interactions among adsorbent and metal ions in solution. A similar tendency was noticed by Lu et al. [43] for the adsorption of Cu^{2+} by walnut shell at optimum pH of 5.0, and Hokkanen et al. [38] reported the optimum pH for Cd(II), Cu(II) and Ni(II) adsorption by amino modified nanostructured microfibrillated cellulose (APS/MFC) was found to be in the pH range of 4–6.

3.2. Effects of preparation conditions

3.2.1. Effect of PEI concentration on adsorption of Cu^{2+}

The effect of the PEI concentration, one of the most important parameters for MSCP preparation, on adsorption of Cu^{2+} by MSCP was studied and the results are shown in Fig. 5. When the PEI concentration was less than 20%, the removal efficiency of Cu^{2+} increased with the increase of PEI concentration. However, with the increase of PEI concentration from 20% to 40%, the removal efficiency of Cu^{2+} on MSCP decreased. The reason for this phenomenon is that polyethylenimine contains many primary and secondary amine groups in its linear polymer

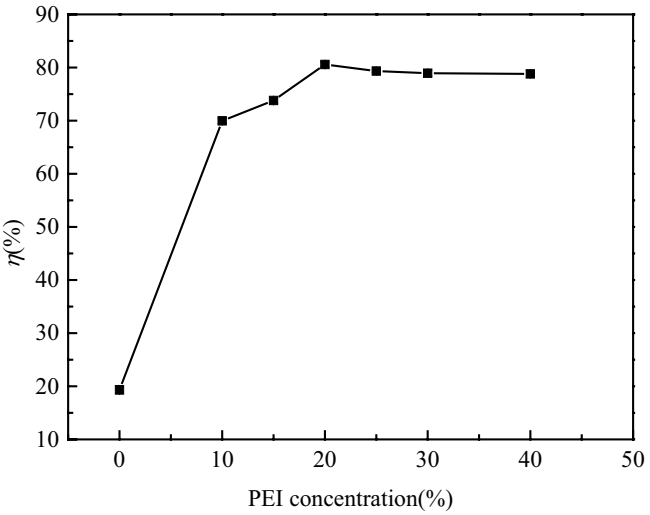

Fig. 5. Effect of PEI concentration (glutaraldehyde concentration = 1.5%; reaction temperature = 298.15 K; ball milling time = 20 min) on the adsorption of Cu^{2+}.

chains and has a strong chelation and adsorption capacity for heavy metal ions. Therefore, with the increase of PEI concentration, the active sites on the surface of MSCP also increased, resulting in the removal efficiency of Cu^{2+} increased. But when the PEI concentration too high (over 20%) can lead to an excessive reaction of MSC with PEI, which further increases the crosslinking density of the polymer network and the resistance of heavy metal ions diffusing into the polymer gel network eventually leads to the decrease of the removal efficiency of Cu^{2+}. When PEI concentration was 20%, the highest removal efficiency of Cu^{2+} by MSCP was 80.57%. Hence, 20% was selected as the optimum PEI concentration for MSCP preparation.

3.2.2. Effect of glutaraldehyde concentration on adsorption of Cu^{2+}

The effect of glutaraldehyde concentration on the adsorption of Cu^{2+} on MSCP is shown in Fig. 6. With the increasing glutaraldehyde concentration from 1.5% to 2.0%, the removal efficiency of Cu^{2+} increased from 80.57% to 83.20%. When glutaraldehyde concentration was over 2.0%, the removal efficiency of Cu^{2+} decreased, and the removal efficiency of Cu^{2+} was only 65.00% at the glutaraldehyde concentration of 3.5%. The glutaraldehyde molecule has two aldehyde groups, which can crosslink with MSC and PEI to form a polymer network with the Schiff base group. As the Schiff base (C=N) group generated by the crosslinking reaction can absorb heavy metal ions, the adsorption sites of MSCP increased with the increase of glutaraldehyde concentration, so the removal efficiency of Cu^{2+} increased. However, when glutaraldehyde concentration was too large, the crosslinking density and the rigidity of the polymer network could be significantly increased, which was not conducive to the extension of the polymer network, and finally leads to the removal efficiency of Cu^{2+} by MSCP decreased. Hence, 2.0% was selected as the optimum glutaraldehyde concentration for MSCP preparation.

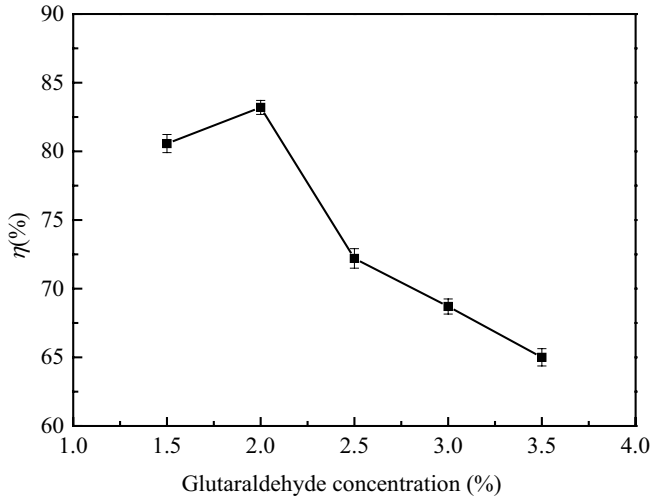

Fig. 6. Effect of glutaraldehyde concentration (PEI concentration = 20%; reaction temperature = 298.15 K; ball milling time = 20 min) on the adsorption of Cu^{2+}.

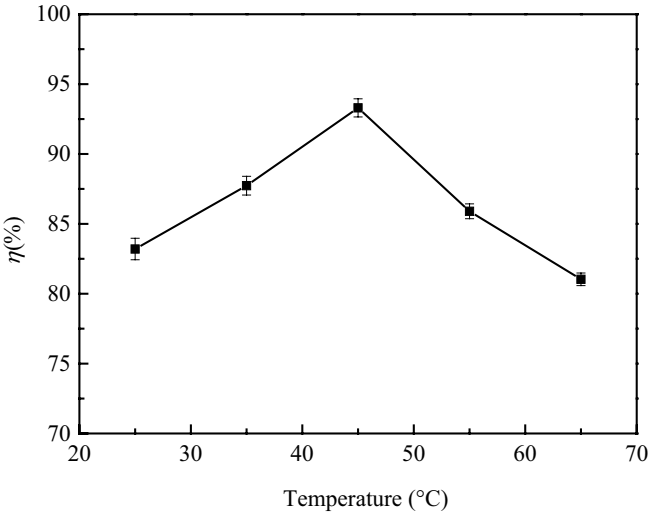

Fig. 7. Effect of reaction temperature (glutaraldehyde concentration = 2.0%; PEI concentration = 20%; ball milling time = 20 min) on the adsorption of Cu^{2+}.

3.2.3. Effect of reaction temperature on adsorption of Cu^{2+}

As shown in Fig. 7, the removal efficiency of Cu^{2+} increased with the increase of the reaction temperature from 298.15 to 318.15 K. The increase of temperature provided more energy for the crosslinking reaction between MSC and PEI, which facilitated the complete reaction of functional groups on MSC and PEI. When the reaction temperature was over 318.15 K, the removal efficiency of Cu^{2+} gradually decreased. This is because too high reaction temperature increased the density of the network structure of MSCP formed by the crosslinking reaction, which was not conducive to the diffusion of Cu^{2+} from the solution into the internal pores of MSCP. Hence, the reaction temperature of 318.15 K was chosen for further experiments.

3.2.4. Effect of ball milling time on adsorption of Cu^{2+}

The effect of ball milling time on the adsorption of Cu^{2+} by MSCP is presented in Fig. 8. With the increase of ball milling time, the removal efficiency of Cu^{2+} increased until 20 min and decreased gradually after the ball milling time exceeds 20 min. The removal efficiency of Cu^{2+} was 63.3% for the adsorbent without ball milling treatment, but increased to 93.3% for the adsorbent after 20 min of ball milling treatment, indicating that ball milling had a significant influence on the adsorption performance of MSCP. With the increase of ball milling time, the crystalline structure of SC was destroyed and the degree of crystallinity of SC was also decreased, which is conducive to the crosslinking reaction between SC and PEI. However, too long ball milling time could destroy the structure of SC, leading to a decrease of removal efficiency of Cu^{2+}. Hence, the ball milling of 20 min was chosen in further experiments.

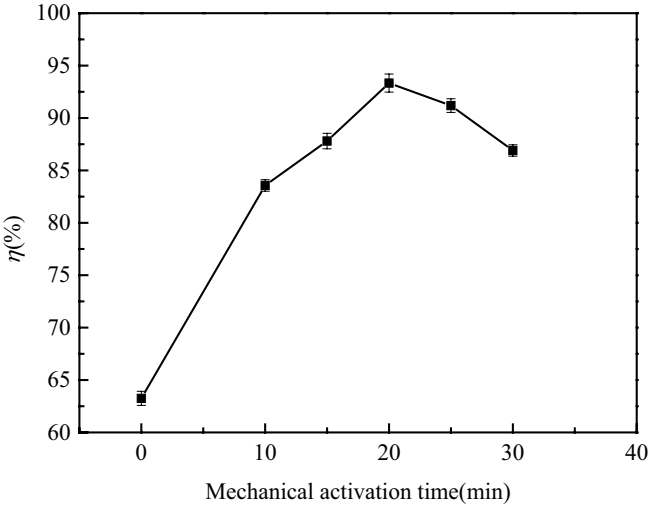

Fig. 8. Effect of ball milling time (glutaraldehyde concentration = 2.0%; PEI concentration = 20%; reaction temperature = 318.15 K) on the adsorption of Cu^{2+}.

3.3. Adsorption isotherms

The adsorption equilibrium results were fitted using the Langmuir and Freundlich models, which were expressed as follows:

$$\frac{C_e}{q_e} = \frac{C_e}{q_m} + \frac{1}{K_L q_m} \tag{4}$$

$$\log q_e = \left(\frac{1}{\mathrm{n}}\right)\log C_e + \log K_F \tag{5}$$

where q_m (mg/g) is the maximum adsorption capacity, q_e (mg/g) is the equilibrium adsorption capacity, K_L (L/mg) is the Langmuir constant, and K_F ((mg/g)(L/mg)$^{1/n}$) and $1/n$ are the Freundlich constants [44].

The Langmuir and Freundlich isotherm models are presented in Fig. 9. Isotherm parameters for adsorption of Cu^{2+}, Pb^{2+} and Zn^{2+} on MSCP are summarized in Table 3. The values of correlation coefficients R^2 revealed that the Langmuir

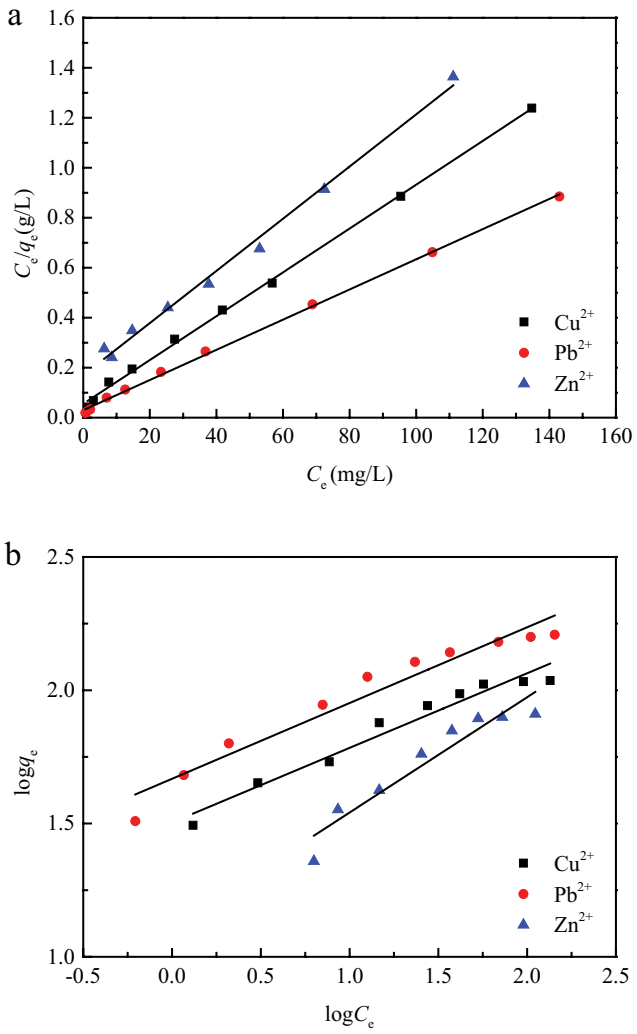

Fig. 9. (a) Plot of Langmuir adsorption isotherm and (b) plot of Freundlich adsorption isotherm.

isotherm model fits better with the experimental data than the Freundlich isotherm model. This indicates that the adsorption of Cu^{2+}, Pb^{2+} and Zn^{2+} by MSCP were monolayer adsorption on the homogeneous surface.

The comparison of the maximum adsorption capacity with some recent different adsorbents toward Cu^{2+}, Pb^{2+} and Zn^{2+} are shown in Table 4 [45–56]. As can be seen in Table 4, MXene and MXene based composites had a high adsorption capacity for Pb^{2+}, but the synthesis method of MXenes is complicated and the cost is high. In addition, MXenes can easily be oxidized in the presence of water and degrade under different conditions, and the acute toxicity of MXenes and their possible environmental risks should be thoroughly considered. After adsorption it is really tedious to separate the MXenes from the solution, which limit them in-field practical utility for the separation of metals/heavy metals from the greater volume of solutions [57]. Although nanocomposite hydrogels are a good bio-absorbent materials for environmental detoxification, its adsorption capacity for Cu^{2+}, Pb^{2+} and Zn^{2+} is generally not high and the poor mechanical properties of the hydrogels

Table 3
Constants of isotherm model

Isotherm models	Isotherm parameters	Values		
		Cu^{2+}	Pb^{2+}	Zn^{2+}
Langmuir	q_m (mg/g)	114.02	165.56	95.79
	K_L (L/mg)	0.16	0.20	0.06
	R^2	0.9983	0.9986	0.9920
Freundlich	K_F ((mg/g)(1/mg)$^{1/n}$)	31.91	46.54	12.84
	n	3.57	3.52	2.31
	R^2	0.9535	0.9401	0.8981

inhibit their applications [58]. Compared with MXenes and nanocomposite hydrogels, MSCP is an environmentally friendly bio-adsorbent prepared by using agricultural waste as raw materials. The preparation process is simple and cost is low. After adsorption, MSCP can be easily separated from aqueous solution through filtration. This data clearly clarified that the MSCP can be used as a very efficient adsorbent to remove Cu^{2+}, Pb^{2+} and Zn^{2+}.

3.4. Adsorption kinetics

The adsorption kinetics results were fitted by the pseudo-first-order model and pseudo-second-order model, which were expressed as follows:

$$\ln\frac{q_e}{q_e - q_t} = k_1 t \tag{6}$$

$$\frac{t}{q_t} = \frac{1}{k_2 q_e^2} + \frac{t}{q_e} \tag{7}$$

where q_t (mg/g) is the adsorption amount of metals on MSCP at time t, k_1 (min^{-1}) and k_2 (g/(mg min)) are the rate constants for pseudo-first-order and pseudo-second-order, respectively [26].

The pseudo-first-order model and pseudo-second-order model are presented in Fig. 10. The rate constant and experimental data of kinetic models are shown in Table 5. Based on the results, the correlation coefficient values ($R^2 > 0.99$) of the pseudo-second-order model are higher than pseudo-first-order and also calculated values of q_e ($q_{e,cal}$) agree with experimental values. This suggests that the adsorption of Cu^{2+}, Pb^{2+} and Zn^{2+} by MSCP follows pseudo-second-order model and the adsorption involved complexation mechanism [45], which was also verified by FTIR analysis and elemental analysis results.

3.5. Competitive adsorption experiments

The competitive adsorption results of MSCP are shown in Fig. 11. When the initial concentration of Cu^{2+}, Pb^{2+} and Zn^{2+} were all 80 mg/L, the adsorption capacities of MSCP for Cu^{2+}, Pb^{2+} and Zn^{2+} in the single metal solution were 87.53, 112.33 and 70.50 mg/g, respectively. The adsorption capacity of MSCP for Cu^{2+}, Pb^{2+} and Zn^{2+} in the multiple

Table 4
Comparison of adsorption capacity of heavy metals by various adsorbents reported in literatures

Adsorbents	q_e (mg/g)			References
	Cu^{2+}	Pb^{2+}	Zn^{2+}	
Corn silk (raw)	15.35		13.98	[45]
Ulvan dialdehyde-gelatin hydrogels	14		6	[46]
Poly(vinylpyrrolidone) hydrogel	86.6		32.20	[47]
Poly(vinylpyrrolidone-*co*-methylacrylate) hydrogels	98.53		61.94	[47]
Poly(vinyl alcohol) and carboxymethyl cellulose composite hydrogels	5.5		5.3	[48]
Conjugate adsorbent		188.67		[49]
Ti(IV) iodovanadate cation exchanger (TIV)		63.29		[50]
$Ti_3C_2T_X$-KH570		147.29		[51]
Enzymatic hydrolysis lignin functionalized Ti_2CT_X MXene		232.9		[52]
MXene/alginate composites	87.6	382.7		[53]
Nanocomposite adsorbent	173.62			[54]
Magnetic graphene oxide composite	62.73			[55]
Magnetic maghemite (c-Fe_2O_3) nanotubes	111.11	71.42	84.95	[56]
MSCP	114.02	165.56	95.79	This study

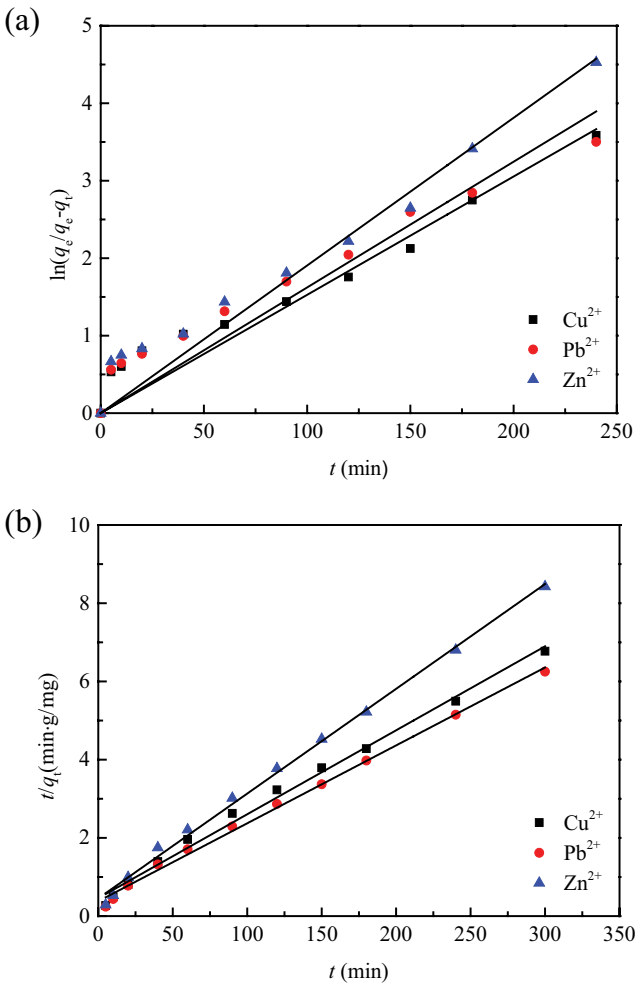

Fig. 10. (a) Plot of pseudo-first-order kinetic model and (b) plot of pseudo-second-order kinetic model.

Table 5
Constants of adsorption kinetics

Kinetic models	Kinetic constants	Values		
		Cu^{2+}	Pb^{2+}	Zn^{2+}
Pseudo-first-order	k_1 (min^{-1})	0.0153	0.0162	0.0191
	R^2	0.9700	0.9670	0.9777
	$q_{e,exp}$ (mg/g)	44.93	48.07	35.67
Pseudo-second-order	$q_{e,cal}$ (mg/g)	46.58	50.20	37.33
	k_2 (g/(mg min))	0.0010	0.0010	0.0016
	R^2	0.9922	0.9957	0.9960

metal solutions decreased significantly compared with that in the single metal solution. In the Cu/Pb and Cu/Zn solutions, the adsorption capacities of Cu^{2+} under the initial concentration of 80 mg/L were 56.75 and 58.25 mg/g, respectively. The results showed that the presence of Pb^{2+} and Zn^{2+} inhibited Cu^{2+} adsorption by MSCP. In the Pb/Cu and Pb/Zn solutions, the adsorption capacities of Pb^{2+} were 69.25 and 108.74 mg/g, indicating that the presence of Cu^{2+} significantly reduced the adsorption capacity of MSCP for Pb^{2+}, while the presence of Zn^{2+} had little effect on the adsorption capacity of Pb^{2+}. As shown in Fig. 11c, in the Zn/Cu and Zn/Pb solutions, the adsorption capacities of Zn^{2+} were 35.17 and 43.17 mg/g, indicating that the presence of Pb^{2+} and Cu^{2+} significantly reduced the adsorption capacity of MSCP for Zn^{2+}. In the ternary metal solution, the adsorption capacities of MSCP were 74.83, 52.83, and 29.67 mg/g for Pb^{2+}, Cu^{2+}, and Zn^{2+}, respectively, and the order of adsorption capacities followed $Pb^{2+} > Cu^{2+} > Zn^{2+}$. The reason was not only related to the specific surface characteristics of MSCP, but also related to the characteristics of these heavy metals [1,7].

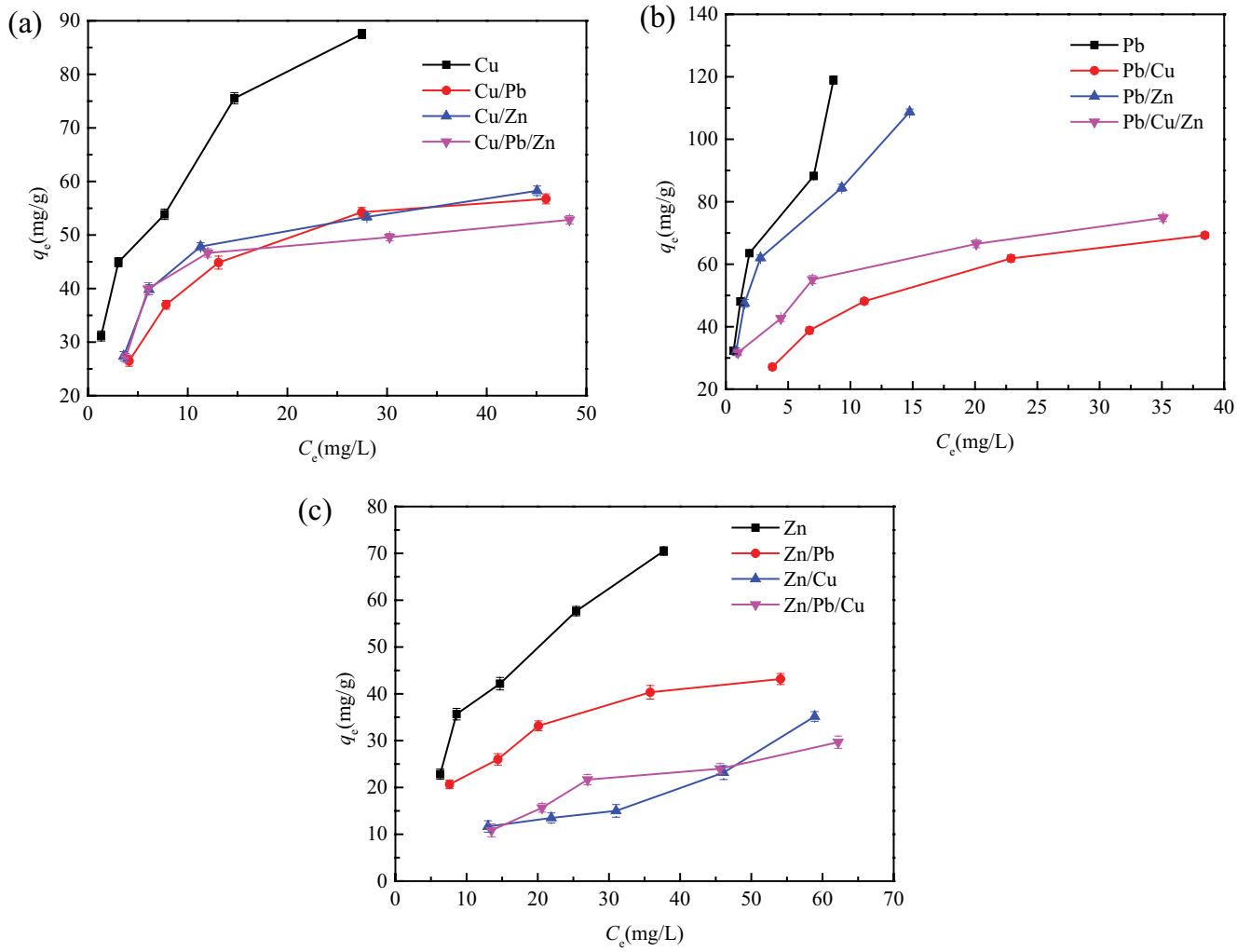

Fig. 11. Single metal solution and multi-metal solution adsorption for (a) Cu^{2+}, (b) Pb^{2+}, and (c) Zn^{2+} by MSCP (MSCP dosage = 0.03 g; T = 298.15 K; time = 390 min).

Table 6
Distribution coefficients and basic characteristics of the three metal ions

Metal ions	Atomic weight	Hydrated ionic radii (Å)	Electronegativity	Ionic radii (Å)	K_d (mL/g)		References
					Single metal solution	Ternary metal solution	
Pb	207.2	4.01	2.33	1.20	30,231	7,920	[59]
Cu	63.54	4.19	1.90	0.72	7,014	2,884	[60]
Zn	65.38	4.30	1.65	0.74	2,868	802	[7]

In multi-solute system, the retention capacity of adsorbents for different metals is commonly compared by distribution coefficient (K_d) [59]. In order to further explore the adsorption selectivity of MSCP for Cu^{2+}, Pb^{2+} and Zn^{2+} metal ions, the value of K_d is used to determine the adsorption selectivity of the three metals. In this study, the retention ability of the three metal ions in multi-solute system were determined by K_d values at the initial concentration of 40 mg/L for Cu^{2+}, Pb^{2+} and Zn^{2+}. The results of K_d and basic characteristics of Cu^{2+}, Pb^{2+} and Zn^{2+} were listed in Table 6 [7,59,60]. In the single metal solution, the K_d values of Cu^{2+}, Pb^{2+} and Zn^{2+} are 7,014; 30,231 and 2,868 mL/g, respectively. Among the three metals, the K_d value of Pb^{2+} (30,231 mL/g) was the highest, indicating that its retention ability was superior to Cu^{2+}, followed by Zn^{2+}. In the ternary metal solution, the K_d values of Cu^{2+}, Pb^{2+} and Zn^{2+} are 2,884; 7,920 and 802 mL/g, respectively. Those results suggested that the order of retention ability of the three metals in the single and ternary metal solution was as follows:

$Pb^{2+} > Cu^{2+} > Zn^{2+}$. Zhu et al. [61], Cutillas-Barreiro et al. [62] and Wu et al. [63] also reported similar orders of adsorption. The quantity of adsorbed ions on the MSCP is related not only to the characteristics of adsorbents but also other factors, such as the hydrated ionic radii, electronegativity, and ionic radii of metal ions. According to previous studies, small radius and high electronegativity of metal ions promote adsorption. The hydrated ionic radii of Pb^{2+}, Cu^{2+}, and Zn^{2+} are 4.01, 4.19 and 4.30 Å, respectively. The small hydrated ionic radii of Pb^{2+} formed smaller three-dimensional hydrated metal clusters or metal hydration shells. The relative weak pore plugging ability enables Pb^{2+} to interact more closely with the adsorbent. The ionic radii of Pb^{2+}, Cu^{2+}, and Zn^{2+} are 1.20, 0.72, and 0.74 Å, respectively, and the electronegativity of Pb^{2+}, Cu^{2+}, and Zn^{2+} are 2.33, 1.90, and 1.65, respectively. The smaller ionic radius and higher electronegativity of Pb^{2+} led to a stronger electronic attractive force between MSCP and Pb^{2+}. Thus, Pb^{2+} is in favor of adsorption on MSCP in multi-metal solutions.

4. Conclusions

The effects of preparation parameters on the adsorption property of MSCP were studied, and the competitive adsorption of Cu^{2+}, Pb^{2+} and Zn^{2+} by MSCP were analyzed in detail. FTIR results and elemental analysis revealed PEI was successfully grafted to the surface of sugarcane bagasse cellulose with glutaraldehyde as a bridge and the possible adsorption mechanism were complexation between heavy metals and $–NH_2$ groups of MSCP. It was found that all the parameters including the PEI concentration, the glutaraldehyde concentration, the reaction temperature, and ball milling time, showed significant effects on the adsorption property of the prepared MSCP. When the PEI concentration was 20%, the glutaraldehyde concentration was 2.0%, the reaction temperature was 318.15 K, and the ball milling time was 20 min, the removal efficiency of Cu^{2+} reached 93.3%. Equilibrium data best fitted to Langmuir isotherm model suggesting monolayer adsorption of Cu^{2+}, Pb^{2+} and Zn^{2+} by MSCP. The maximum adsorption capacities for Cu^{2+}, Pb^{2+} and Zn^{2+} were 114.02, 165.56 and 95.79 mg/g, respectively. experimental data for Cu^{2+}, Pb^{2+} and Zn^{2+} adsorption by MSCP were best fitted to pseudo-second-order kinetic model indicating involvement of complexation mechanism. In multi-solute system, the competitive adsorption ability of heavy metals by MSCP followed the order of $Pb^{2+} > Cu^{2+} > Zn^{2+}$. The results of this study showed that the sugarcane bagasse after modified by PEI had high adsorption capacity and can be used as low-cost and efficient adsorbent to remove Cu^{2+}, Pb^{2+} and Zn^{2+} from aqueous solutions.

Acknowledgements

This work was supported by the National Natural Science Foundation of China (31860014), Natural Science Foundation of Guangxi Province (2020GXNSFAA259051 and 2021GXNSFBA196028), and Special Project for Basic Scientific Research of Guangxi Academy of Agricultural Sciences (GNK2021YT137).

Author disclosure statement

The authors declare no conflicts of interest.

References

[1] X.S. Wang, H.H. Miao, W. He, H.L. Shen, Competitive adsorption of Pb(II), Cu(II), and Cd(II) ions on wheat-residue derived black carbon, J. Chem. Eng. Data, 56 (2011) 444–449.
[2] S. Gullipilli, R.B. Rupakula, Adsorption studies of Cr(VI) and Cu(II) metal ions from aqueous solutions by synthesized Ag and Mg co-doped TiO_2 nanoparticles, Sep. Sci. Technol., 54 (2019) 2983–2992.
[3] S. Tighadouini, S. Radi, M. Bacquet, S. Degoutin, M. Zaghrioui, S. Jodeh, I. Warad, Removal efficiency of Pb(II), Zn(II), Cd(II) and Cu(II) from aqueous solution and natural water by ketoenol–pyrazole receptor functionalized silica hybrid adsorbent, Sep. Sci. Technol., 52 (2017) 608–621.
[4] Y.-Y. Wang, Y.-X. Liu, H.-H. Lu, R.-Q. Yang, S.-M. Yang, Competitive adsorption of Pb(II), Cu(II), and Zn(II) ions onto hydroxyapatite-biochar nanocomposite in aqueous solutions, J. Solid State Chem., 261 (2018) 53–61.
[5] A. Anjum, C.K. Seth, M. Datta, Removal of As^{3+} using chitosan–montmorillonite composite: sorptive equilibrium and kinetics, Adsorpt. Sci. Technol., 31 (2013) 303–324.
[6] Z. Mahdi, Q.J. Yu, A. El Hanandeh, Competitive adsorption of heavy metal ions (Pb^{2+}, Cu^{2+}, and Ni^{2+}) onto date seed biochar: batch and fixed bed experiments, Sep. Sci. Technol., 54 (2019) 888–901.
[7] İ. Ayhan Şengil, M. Özacar, Competitive biosorption of Pb^{2+}, Cu^{2+} and Zn^{2+} ions from aqueous solutions onto valonia tannin resin, J. Hazard. Mater., 166 (2009) 1488–1494.
[8] M.Y. Pamukoglu, M.C. Karabuga, Removal of Cr(III) ions from wastewater by using ligand adsorption, Environ. Eng. Sci., 35 (2018) 703–709.
[9] S.M.S. Li, M.Q. Qiu, Z.X. Zeng, W.L. Xue, Effective modified walnut shell adsorbent: synthesis and adsorption behavior for Pb^{2+} and Ni^{2+} from aqueous solution, Environ. Eng. Sci., 36 (2019) 1421–1432.
[10] J. Dutta, A.A. Mala, Removal of antibiotic from the water environment by the adsorption technologies: a review, Water Sci. Technol., 82 (2020) 401–426.
[11] C.Y. Cao, B. Yu, M. Wang, Y.Y. Zhao, Y.H. Zhao, Adsorption properties of Pb^{2+} on thermal-activated serpentine, Sep. Sci. Technol., 54 (2019) 3037–3045.
[12] J. Junthip, W. Promma, S. Sonsupap, C. Boonyanusith, Adsorption of paraquat from water by insoluble cyclodextrin polymer crosslinked with 1,2,3,4-butanetetracarboxylic acid, Iran. Polym. J., 28 (2019) 213–223.
[13] Q.Y. Lin, Q.H. Wang, Y.X. Duan, X.P. Wei, G.R. Wu, Y.H. Luo, Q.L. Xie, Removal of Cu(II), Cr(III), and Cr(VI) from aqueous solution using a novel agricultural waste adsorbent, Sep. Sci. Technol., 48 (2013) 2843–2851.
[14] K.A. Krishnan, K.G. Sreejalekshmi, V. Vimexen, V.V. Dev, Evaluation of adsorption properties of sulphurised activated carbon for the effective and economically viable removal of Zn(II) from aqueous solutions, Ecotoxicol. Environ. Saf., 124 (2016) 418–425.
[15] S.K. Zhou, Y.J. Liu, H.Y. Jiang, W.J. Deng, G.M. Zeng, Adsorption of U(VI) from aqueous solution by a novel chelating adsorbent functionalized with amine groups: equilibrium, kinetic, and thermodynamic studies, Environ. Eng. Sci., 35 (2018) 53–61.
[16] V.K. Gupta, A. Nayak, S. Agarwal, Bio-adsorbents for remediation of heavy metals: current status and their future prospects, Environ. Eng. Res., 20 (2016) 1–18.
[17] S. Ai, Y.C. Huang, T.H. Xie, C.D. Huang, Facile carboxylation of sugarcane bagasse and the adsorption mechanism for cadmium ions, Ind. Eng. Chem. Res., 59 (2020) 8795–8804.
[18] A.K. Chandel, S.S. da Silva, W. Carvalho, O.V. Singh, Sugarcane bagasse and leaves:foreseeable biomass of biofuel and bio-products, J. Chem. Technol. Biotechnol., 87 (2012) 11–20.

[19] W.S. Wan Ngah, M.A.K.M. Hanafiah, Removal of heavy metal ions from wastewater by chemically modified plant wastes as adsorbents: a review, Bioresour. Technol., 99 (2008) 3935–3948.
[20] S.N.C. Ramos, A.L.P. Xavier, F.S. Teodoro, L.F. Gil, L.V.A. Gurgel, Removal of cobalt(II), copper(II), and nickel(II) ions from aqueous solutions using phthalate-functionalized sugarcane bagasse: mono-and multicomponent adsorption in batch mode, Ind. Crops Prod., 79 (2016) 116–130.
[21] A. Nashine, A. Tembhurkar, Iron oxide impregnated sugarcane bagasse waste material as sorbent for As(III) removal from water: kinetic, equilibrium and thermodynamic studies, J. Water Supply Res. Technol. AQUA, 69 (2020) 99–112.
[22] Y.N. Chen, M.F. He, C.Z. Wang, Y.M. Wei, A novel polyvinyltetrazole-grafted resin with high capacity for adsorption of Pb(II), Cu(II) and Cr(III) ions from aqueous solutions, J. Mater. Chem. A, 2 (2014) 10444–10453.
[23] M.R. Huang, H.J. Lu, X.G. Li, Synthesis and strong heavy-metal ion sorption of copolymer microparticles, J. Mater. Chem., 22 (2012) 17685–17699.
[24] Y. Pang, G. Zeng, L. Tang, Y. Zhang, Y. Liu, X. Lei, Z. Li, J. Zhang, G. Xie, PEI grafted magnetic porous powder for highly effective adsorption of heavy metal ions, Desalination, 281 (2011) 278–284.
[25] Y. Ma, W.J. Liu, N. Zhang, Y.S. Li, H. Jiang, G.P. Sheng, Polyethylenimine modified biochar adsorbent for hexavalent chromium removal from the aqueous solution, Bioresour. Technol., 169 (2014) 403–408.
[26] Y.J. Shi, T. Zhang, H.Q. Ren, A. Kruse, R.F. Cui, Polyethylene imine modified hydrochar adsorption for chromium(VI) and nickel(II) removal from aqueous solution, Bioresour. Technol., 247 (2018) 370–379.
[27] H.M. Jiang, M.L. Sun, J.Y. Xu, A.M. Lu, Y. Shi, Magnetic Fe_3O_4 nanoparticles modified with polyethyleneimine for the removal of Pb(II), Clean–Soil Air Water, 44 (2016) 1146–1153.
[28] H.J. Liu, Y.C. Zhou, Y.B. Yang, K. Zou, R.J. Wu, K. Xia, S.B. Xie, Synthesis of polyethylenimine/graphene oxide for the adsorption of U(VI) from aqueous solution, Appl. Surf. Sci., 471 (2019) 88–95.
[29] P. Phanthong, P. Reubroycharoen, X.G. Hao, G.W. Xu, A. Abudula, G.Q. Guan, Nanocellulose: extraction and application, Carbon Resour. Convers., 1 (2018) 32–43.
[30] M. Rahimi Kord Sofla, R.J. Brown, T. Tsuzuki, T.J. Rainey, A comparison of cellulose nanocrystals and cellulose nanofibres extracted from bagasse using acid and ball milling methods, Adv. Nat. Sci.: Nanosci. Nanotechnol., 7 (2016) 035004.
[31] Md. Nuruddin, M. Hosur, Md. Jamal Uddin, D. Baah, S. Jeelani, A novel approach for extracting cellulose nanofibers from lignocellulosic biomass by ball milling combined with chemical treatment, J. Appl. Polym. Sci., 133 (2016) e42990, doi: 10.1002/app.42990.
[32] W.Y. Jiang, Y.H. Xing, L.Y. Zhang, X.M. Guo, Y.W. Lu, M. Yang, J. Wang, G.T. Wei, Polyethylenimine-modified sugarcane bagasse cellulose as an effective adsorbent for removing Cu(II) from aqueous solution, J. Appl. Polym. Sci., 138 (2021) e49830, doi: 10.1002/app.49830.
[33] H.S. Qi, C.Y. Chang, L. Zhang, Properties and applications of biodegradable transparent and photoluminescent cellulose films prepared via a green process, Green Chem., 11 (2009) 177–184.
[34] N. Djebri, M. Boutahala, N.E. Chelali, N. Boukhalfa, L. Zeroual, Enhanced removal of cationic dye by calcium alginate/organobentonite beads: modeling, kinetics, equilibriums, thermodynamic and reusability studies, Int. J. Biol. Macromol., 92 (2016) 1277–1287.
[35] D.R. Mulinari, H.J.C. Voorwald, M.O.H. Cioffi, M.L.C.P. Da Silva, S.M. Luz, Preparation and properties of HDPE/sugarcane bagasse cellulose composites obtained for thermokinetic mixer, Carbohydr. Polym., 75 (2009) 317–321.
[36] G.R. Xie, X.Q. Shang, R.F. Liu, J. Hu, S.F. Liao, Synthesis and characterization of a novel amino modified starch and its adsorption properties for Cd(II) ions from aqueous solution, Carbohydr. Polym., 84 (2011) 430–438.
[37] A.Q. Dong, J. Xie, W.M. Wang, L.P. Yu, Q. Liu, Y.P. Yin, A novel method for amino starch preparation and its adsorption for Cu(II) and Cr(VI), J. Hazard. Mater., 81 (2011) 448–454.
[38] S. Hokkanen, E. Repo, T. Suopajärvi, H. Liimatainen, J. Niinimaa, M. Sillanpää, Adsorption of Ni(II), Cu(II) and Cd(II) from aqueous solutions by amino modified nanostructured microfibrillated cellulose, Cellulose, 21 (2014) 1471–1487.
[39] A. Benhouria, M.A. Islam, H. Zaghouane-Boudiaf, Calcium alginate–bentonite–activated carbon composite beads as highly effective adsorbent for methylene blue, Chem. Eng. J., 270 (2015) 621–630.
[40] R.N. Li, Z.W. Wang, X.T. Zhao, X. Li, X.Y. Xie, Magnetic biochar-based manganese oxide composite for enhanced fluoroquinolone antibiotic removal from water, Environ. Sci. Pollut. Res., 25 (2018) 31136–31148.
[41] K.A.G. Gusmao, L.V.A. Gurgel, T.M.S. Melo, L.F. Gil, Application of succinylated sugarcane bagasse as adsorbent to remove methylene blue and gentian violet from aqueous solutions – kinetic and equilibrium studies, Dyes Pigm., 92 (2012) 967–974.
[42] D.D. Reddy, R.K. Ghosh, J.P. Bindu, M. Mahadevaswamy, Removal of methylene blue from aqueous system using tobacco stems biomass: kinetics, mechanism and single-stage adsorber design, Environ. Prog. Sustainable Energy, 36 (2017) 1005–1012.
[43] X.G. Lu, P.P. Yan, X.F. Dang, Adsorption of Cu^{2+} from aqueous solution by walnut shell, Adv. Mater. Res., 864–867 (2014) 1327–1332.
[44] W.Y. Jiang, L.Y. Zhang, X.M. Guo, M. Yang, Y.W. Lu, Y.J. Wang, Y.S. Zheng, G.T. Wei, Adsorption of cationic dye from water using an iron oxide/activated carbon magnetic composites prepared from sugarcane bagasse by microwave method, Environ. Technol., 42 (2021) 337–350.
[45] M. Petrović, T. Šoštarić, M. Stojanović, J. Petrović, M. Mihajlović, A. Cosović, S. Stanković, Mechanism of adsorption of Cu^{2+} and Zn^{2+} on the corn silk (*Zea mays* L.), Ecol. Eng., 99 (2017) 83–90.
[46] N. Wahlström, S. Steinhagen, G. Toth, H. Pavia, U. Edlund, Ulvan dialdehyde-gelatin hydrogels for removal of heavy metals and methylene blue from aqueous solution, Carbohydr. Polym., 249 (2020) 116841, doi: 10.1016/j.carbpol.2020.116841.
[47] Ö.F. Kemik, F.A. Ngwabebhoh, U. Yildiz, A response surface modelling study for sorption of Cu^{2+}, Ni^{2+}, Zn^{2+} and Cd^{2+} using chemically modified poly(vinylpyrrolidone) and poly(vinylpyrrolidone-*co*-methylacrylate) hydrogels, Adsorpt. Sci. Technol., 35 (2017) 263–283.
[48] L.Y. Wang, M.J. Wang, Removal of heavy metal ions by poly(vinyl alcohol) and carboxymethyl cellulose composite hydrogels prepared by a freeze-thaw method, ACS Sustainable Chem. Eng., 4 (2016) 2830–2837.
[49] Md. Rabiul Awual, Assessing of lead(II) capturing from contaminated wastewater using ligand doped conjugate adsorbent, Chem. Eng. J., 289 (2016) 65–73.
[50] Mu. Naushad, Z.A. ALOthman, Md.R. Awual, M.M. Alam, G.E. Eldesoky, Adsorption kinetics, isotherms, and thermodynamic studies for the adsorption of Pb^{2+} and Hg^{2+} metal ions from aqueous medium using Ti(IV) iodovanadate cation exchanger, Ionics, 21 (2015) 2237–2245.
[51] D. Gan, Q. Huang, J. Dou, H. Huang, J. Chen, M. Liu, Y. Wen, Z. Yang, X. Zhang, Y. Wei, Bioinspired functionalization of MXenes ($Ti_3C_2T_X$) with amino acids for efficient removal of heavy metal ions, Appl. Surf. Sci., 504 (2020) 144603, doi: 10.1016/j.apsusc.2019.144603.
[52] S. Wang, Y. Liu, Q.-F. Lü, H. Zhuang, Facile preparation of biosurfactant-functionalized Ti_2CT_X MXene nanosheets with an enhanced adsorption performance for Pb(II) ions, J. Mol. Liq., 297 (2020) 111810, doi: 10.1016/j.molliq.2019.111810.
[53] Y. Dong, D. Sang, C. He, X. Sheng, L. Lei, MXene/alginate composites for lead and copper ion removal from aqueous solutions, RSC Adv., 9 (2019) 29015–29022.
[54] Md. R. Awual, G.E. Eldesoky, T. Yaita, Mu. Naushad, H. Shiwaku, Z.A. AlOthman, S. Suzuki, Schiff based ligand containing nanocomposite adsorbent for optical copper(II)

ions removal from aqueous solutions, Chem. Eng. J., 279 (2015) 639–647.
[55] X.J. Hu, Y.G. Liu, H. Wang, A.W. Chen, G.M. Zeng, S.M. Liu, Y.M. Guo, X. Hu, T.T. Li, Y.Q. Wang, L. Zhou, S.H. Liu, Removal of Cu(II) ions from aqueous solution using sulfonated magnetic graphene oxide composite, Sep. Purif. Technol., 108 (2013) 189–195.
[56] A. Roy, J. Bhattacharya, Removal of Cu(II), Zn(II) and Pb(II) from water using microwave-assisted synthesized maghemite nanotubes, Chem. Eng. J., 211–212 (2012) 493–500.
[57] T. Rasheed, F. Kausar, K. Rizwan, M. Adeel, F. Sher, N. Alwadai, F.H. Alshammari, Two dimensional MXenes as emerging paradigm for adsorptive removal of toxic metallic pollutants from wastewater, Chemosphere, 287 (2022) 132319, doi: 10.1016/j.chemosphere.2021.132319.
[58] G. Sharma, B. Thakur, Mu. Naushad, A. Kumar, F.J. Stadler, S.M. Alfadul, G.T. Mola, Applications of nanocomposite hydrogels for biomedical engineering and environmental protection, Environ. Chem. Lett., 16 (2018) 113–146.
[59] N. Rahbar, H. Yazdanpanah, Z. Ramezani, M.R. Shushizadeh, M. Enayat, M. Mansourzadeh, Comparative and competitive adsorption of Cu(II), Cd(II) and Pb(II) onto *Sepia pharaonis* endoskeleton biomass from aqueous solutions, Water Environ. J., 32 (2018) 209–216.
[60] M. Arshadi, M.J. Amiri, S. Mousavi, Kinetic, equilibrium and thermodynamic investigations of Ni(II), Cd(II), Cu(II) and Co(II) adsorption on barley straw ash, Water Resour. Ind., 6 (2014) 1–17.
[61] Y. Zhu, J. Hu, J. Wang, Competitive adsorption of Pb(II), Cu(II) and Zn(II) onto xanthate-modified magnetic chitosan, J. Hazard. Mater., 221–222 (2012) 155–161.
[62] L. Cutillas-Barreiro, R. Paradelo, A. Igrexas-Soto, A. Núñez-Delgado, M.J. Fernández-Sanjurjo, E. Álvarez-Rodriguez, G. Garrote, J.C. Nóvoa-Muñoz, M. Arias-Estévez, Valorization of biosorbent obtained from a forestry waste: competitive adsorption, desorption and transport of Cd, Cu, Ni, Pb and Zn, Ecotoxicol. Environ. Saf., 131 (2016) 118–126.
[63] Q. Wu, S. Dong, L. Wang, X. Li, Single and competitive adsorption behaviors of Cu^{2+}, Pb^{2+} and Zn^{2+} on the biochar and magnetic biochar of pomelo peel in aqueous solution, Water, 13 (2021) 868, doi: 10.3390/w13060868.